which is topochemical. The other minor reaction that occurs is:

$$\alpha\text{-B} \rightarrow \beta\text{-B} \qquad (11)$$

Acknowledgment. Work performed under Contract W-7405-eng-26 with the United States Energy Research and Development Administration.

Appendix

For a weight distribution of particles with respect to radius, $F_\omega(r)$, the overall weight gain curves for the topochemical and diffusion controlled mechanisms can be derived. For the topochemical mechanism

$$\mathrm{d}x/\mathrm{d}t = -k \qquad \text{(A)}$$

where x is the instantaneous distance from the center to the reaction front. For the diffusion controlled mechanism

$$\mathrm{d}x/\mathrm{d}t = -k/(r-x) \qquad \text{(B)}$$

The integrated forms of A and B are

$$r - x = kt \text{ for A} \qquad \text{(C)}$$

and

$$r - x = \sqrt{2kt} \text{ for B} \qquad \text{(D)}$$

A parameter τ will be used for both cases to replace kt for eq C and $(2kt)^{1/2}$ for eq D. It will be noted that eq C and D are valid only if $r \geq \tau$.

$$r - x = \tau \qquad r \geqslant \tau \qquad \text{(E)}$$

$$r = 0 \qquad r \leqslant \tau \qquad \text{(F)}$$

The ratio of the weight gain of a particular partial radius at any time, $\omega(t,r)$, to the final weight gain, $\omega(\infty,r)$ is given by

$$\omega(t,r)/\omega(\infty,r) = (r^3 - x^3)/r^3 \qquad \text{(G)}$$

for a solid or

$$\frac{\omega(t,r)}{\omega(\infty,r)} = \frac{3\tau}{r} - \frac{3\tau^2}{r^2} + \frac{\tau^3}{r^3} \qquad \text{for } r \geqslant \tau \qquad \text{(H)}$$

$$\frac{\omega(t,r)}{\omega(\infty,r)} = 1 \qquad \text{for } r \leqslant \tau \qquad \text{(I)}$$

Thus for total weight gain $\omega_\mathrm{T}(t)$ for all the particles one has

$$\frac{\omega_\mathrm{T}(t)}{\omega_\mathrm{T}(\infty)} = F_\omega(\tau) + \int_{r=\tau}^{r_\mathrm{max}} \frac{\partial F_\omega(r)}{\partial r}\left(\frac{3\tau}{r} - \frac{3\tau^2}{r^2} + \frac{\tau^3}{r^3}\right)\mathrm{d}r \qquad \text{(J)}$$

In practice $F_\omega(r)$ was measured at a finite number of radii and could thus be approximated by straight lines between measurements. Therefore, let

$$C_i = \frac{\partial F_\omega(r_{i-1} \text{ (or) } \tau < r \leqslant r_i)}{\partial r} \qquad \text{(K)}$$

and eq J may be integrated to give

$$\frac{\omega_\mathrm{T}(\tau)}{\omega_\mathrm{T}(\infty)} = F_\omega(r_j) + (\tau - r_j)C_j + \sum_{i=j+1} C_i\left[3\tau \ln \frac{r_i}{\max(r_{i-1},\tau)} + 3\tau^2\left(\frac{1}{r_i} - \frac{1}{\max(r_{i-1},\tau)}\right) - \frac{\tau^3}{2}\left(\frac{1}{r_i^2} - \frac{1}{(\max(r_{i-1},\tau))^2}\right)\right] \qquad \text{(L)}$$

where r_j is the highest value bounded by τ ($r_j = r_{i,\mathrm{max}} \leq \tau$).

Registry No. BN, 10043-11-5; B_6N, 59765-75-2; N_2, 7727-37-9; B, 7440-42-8.

References and Notes

(1) J. B. Condon and E. A. Larson, *J. Chem. Phys.*, **59**, 855 (1973).
(2) F. N. Rhines, *Trans. Am. Inst. Min., Metall. Pet. Eng.*, 246 (1940); *J. Corrosion*, 4, 15 (1947).
(3) F. N. Rhines, W. A. Johnson, and W. A. Anderson, *Trans. Am. Inst. Min., Metall. Pet. Eng., Tech. Publ.*, **No. 1368** (1941).
(4) J. B. Condon, "Calculations of Nonspalling Isothermal Hydriding Rates for Uranium", Y-1963, Union Carbide Corporation, Nuclear Division, Oak Ridge Y-12 Plant, Oak Ridge, Tenn., Oct. 1974.
(5) K. Niedenzer and J. W. Dawson, "Boron-Nitrogen Compounds", Academic Press, New York, N.Y., 1965.
(6) V. M. Sleptsov and G. V. Samsonov, *Dopov. Akad. Nauk. Ukr. R.S.R.*, 1116-18 (1959).
(7) H. F. Rizzo, W. C. Simmons, and H. O. Bielstein, *J. Electrochem. Soc.*, **109**, 10795 (1962).
(8) D. R. Petrak and R. Ruh, *Natl. Bur. Stand. (U.S.), Spec. Publ.*, **No. 364**, 605 (1972).
(9) G. V. Samsonov, L. Ya Markovskii, A. F. Zhigaeh, and M. G. Valyashko, "Boron—Its Compounds and Alloys", Publishing House of the Academy of Science of the Ukraninian S.S.R., Kiev, 1960. Available in translation AEC-tr-5032. See p 51.
(10) A. E. Newkirk, *Adv. Chem. Ser.*, **No. 32**, 27-41 (1961).
(11) J. L. Hoard and R. E. Hughes, "The Chemistry of Boron and Its Compounds", E. L. Muetterties, Ed., Wiley, New York, N.Y., 1967, pp 25-154.
(12) C. E. Holcombe, Jr., and O. J. Horne, Jr., *J. Am. Ceram. Soc.*, **55**, 106 (1972).
(13) P. Runow, *J. Mater. Sci.*, **7**, 499-511 (1972).
(14) S. LaPlaca and B. Post, *Planseeber. Pubvermetall.*, **9**, 109 (1961).

Contribution from the Chemistry Division,
Oak Ridge National Laboratory, Oak Ridge, Tennessee 37830

Identification of Polyborate and Fluoropolyborate Ions in Solution by Raman Spectroscopy

L. MAYA

Received March 8, 1976　AIC60182F

The polymeric ions $B_5O_6(OH)_4^-$, $B_3O_3(OH)_4^-$, $B_4O_5(OH)_4^{2-}$, and $B_3O_3F_6^{3-}$ have been identified in solution and their regions of stability established. Comparisons of Raman spectra of the solutions with the spectra of solid reference materials containing the same structural entities, $NaB_5O_8 \cdot 5H_2O$, orthorhombic metaboric acid $(HBO_2)_3$, $Na_2B_4O_7 \cdot 10H_2O$, and $Na_3B_3F_6O_3$ were used to identify the ions. The charge on the polyborate ions was established on the basis of material and ionic balances. The hydrolytic behavior of $Na_3B_3F_6O_3$ was established. This compound is partially depolymerized into $BF_2(OH)_2^-$ ions which disproportionate into BF_3OH^-, F^-, and H_3BO_3. A new synthesis for $Na_3B_3F_6O_3$ was developed.

Introduction

The presence of polyborate ions in solution has been established by cryoscopic methods, nuclear magnetic resonance, ir, conductance, pH titration, and temperature jump techniques. These studies have shown that equilibrium between polyborate species is very fast and changes in equilibrium compositions do not take place. The most extensive work on the subject is that of Ingri[1,2] who postulated, on the basis of

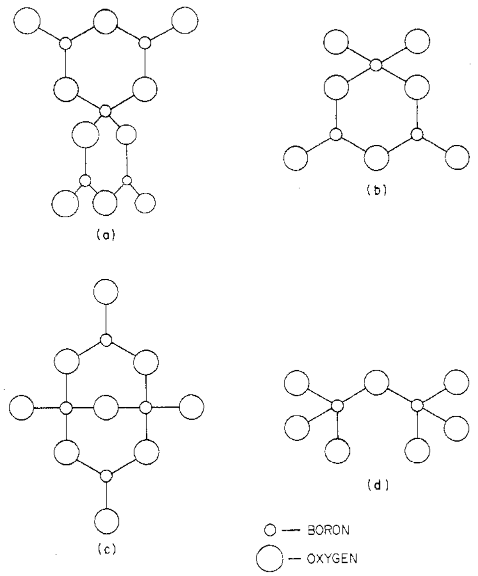

Figure 1. Structural skeletons of polyborate ions: (a) pentaborate; (b) triborate; (c) tetraborate; (d) diborate.

electrometric titrations, the presence of a number of ions which he described by a set of numbers, giving number of boron atoms in the ion and the charge, respectively; these are (1,1), (5,1), (3,1), (4,2), and (3,2). In addition to these, Mesmer, et al.,[3] postulated also on the basis of electrometric titrations from data obtained at 50 and 200 °C the ion (5,3) as an alternative to (4,2) and also a (2,1) ion. Although these studies have been very informative and included the derivation of formation constants, there is no direct evidence about the identity and structure of these ions. Nevertheless, the structures of these ions were inferred[3] on the basis of known structures of crystalline borates for which Christ[4] and also Edwards and Ross[5] have given a set of rules regarding structural parameters. The (3,1) and (3,2) ions are derived from the boroxine skeleton which consists of a six-member ring of alternating oxygen and boron atoms. The (5,1) and (5,3) ions are derived from the pentaborate skeleton which consists of two boroxine rings sharing one boron atom. The (4,2) ion is related to tetraborate, two boroxine rings sharing two boron atoms. Finally the (2,1) ion is related to the structure of pinnoite, a mineral, which has two $B(OH)_3$ groups joined by an oxygen bridge. The structural skeletons of those ions are described in Figure 1.

Raman spectroscopy is ideally suited for the derivation of structural information about ions in solution and indeed attempts were made in the past to study the H_3BO_3–$B(OH)_4^-$ equilibrium, starting with the pioneering work of Hibben[6] and later followed by Laubengayer and Rosenstein.[7] However, their results did not resolve the nature of the polyborate ions, mainly due to the relatively low concentrations involved and the lack of sensitivity of the earlier instrumentation. Mesmer[8] observed by means of Raman spectroscopy peaks other than $B(OH)_3$ and $B(OH)_4^-$ in the pH range 8–10 but no detailed interpretation was made. The purpose of this work was to reexamine the boric acid–borate equilibrium, by taking advantage of the increased sensitivity gained with the advent of lasers as exciting sources. This study was extended to the boric acid–sodium fluoride system. The equilibria involving monomeric species in dilute solutions are well understood[9] but information is lacking about possible polymeric species in more concentrated solutions.

There is a sharp contrast between the extensive work done on the borate systems and the limited knowledge about fluoropolyborates. The only clue as to their possible existence is the fact that a number of solids containing such complex ions have been reported,[10] of which $Na_3B_3F_6O_3$ is representative. It is generally assumed that these compounds are derived from the boroxine ring on the basis of an ir study[11] and the pervasive occurrence of such a structural unit in borates in general.

The approach taken in the present study is similar to that adopted by Edwards et al.[12] in establishing the structure of the borate ion, using, in addition to symmetry considerations, the spectrum of a solid of a known crystal structure to confirm the identity of the ion in solution.

Experimental Section

The Raman spectra were obtained using the beam (600 mW at 488.0 nm) from a Spectra Physics Model 164 argon laser and recorded with a modified Cary 81 spectrophotometer. Carbon tetrachloride was used as a standard to calibrate wavelengths. Samples were held in 7 mm o.d. Pyrex tubing. All spectra were obtained at ambient temperature with the exception of a melt of metaboric acid recorded at 220 °C. The ^{19}F NMR spectra were obtained in a Burke spectrometer operating at 84.67 MHz.

Concentrated solutions, having pH values of 5.0, 6.1, 7.0, 8.0, 9.0, and 10.0, of boric acid–sodium borate at or near the saturation point at 25 °C were prepared by mixing appropriate amounts of boric acid and sodium hydroxide. All the solid materials used for confirmation of spectra were prepared and characterized by chemical analysis and their x-ray powder diffraction patterns with the exception of sodium tetraborate decahydrate which was a commercial product, reagent grade from Allied Chemical. Pinnoite [$Mg(BO_2)_2 \cdot 3H_2O$] was kindly provided by Dr. J. White of the Smithsonian Institution. Preparations of metaboric acid started from reagent grade boric acid crystallized twice from water after treatment with active carbon. (This treatment was necessary to eliminate impurities giving interfering fluorescence in the spectra.) Orthorhombic metaboric acid was prepared by drying boric acid overnight at 110 °C. Monoclinic metaboric acid was prepared by the conversion, at 135 °C, of the orthorhombic form in a sealed tube or directly from boric acid according to the method of Kracek et al.[13] Anhydrous sodium metaborate was prepared by the fusion of boric acid and sodium bicarbonate. Sodium pentaborate, $NaB_5O_8 \cdot 5H_2O$, was crystallized by slow cooling, from 80 to 25 °C, of a solution containing 6.25 wt % Na_2O and 32.3 wt % B_2O_3. The sodium salt of hexafluoroboroxine, $Na_3B_3F_6O_3$, was prepared by Ryss's method.[10] An alternate and simpler method for the preparation of this compound was developed in the course of this work and consisted of the following steps: A 50 ml aqueous solution containing 50 mmol each of H_3BO_3, $NaBF_3OH$, and NaF was filtered after being stirred for 30 min and then concentrated tenfold by distillation under vacuum. The gel-like residue was suspended in 100 ml of absolute ethanol and filtered giving an almost quantitative yield of pure $Na_3B_3F_6O_3$. Anal: Na, 26.0 wt % (theor 26.2%); B, 12.2% (12.3%); and F, 43.9% (43.3%). Sodium hydroxyfluoroborate, $NaBF_3OH$, was prepared according to a method described by Pawlenko.[14]

The Raman spectra of the solutions confirmed the presence of polyborate ions, and their identity was established by comparison with the spectra of the reference solids. After this step, a series of determinations was performed to find the polyborate ion concentration in each solution and also the average proportion of tetrahedral boron in the ions, which is a direct measure of their charge. This was done by the spectrophotometric determination of boric acid and borate present from the intensity of the 875 and 745 cm^{-1} bands, respectively. Standard solutions of boric acid and of sodium metaborate were used to calibrate the intensities. A Pyrex tube, 7 mm o.d., provided with a Teflon stopcock was fixed in position in the laser light path. In each determination, the tube was rinsed three times with the solution to be examined prior to use. Three tracings of each peak were obtained and integrated to obtain an average intensity value. The polyborate ion concentration was derived by the difference of the amount of boron present as boric acid and/or monoborate from the total boron present as determined by titration. The average proportion of tetrahedral boron in the polyborate ions, which is measured by the ratio of sodium to boron, was derived from a material balance of the sodium present. The amount of monoborate determined spectrophotometrically was subtracted from the total alkalinity as determined by titration.

The concentration of the fluoropolyborate ion was estimated from a material balance based on the intensities of the Raman and ^{19}F NMR signals.

Table I. Raman Spectra of Solutions Containing Complex Borate Ions[a]

	Solution								
	pH	[B], mol/l.	Frequencies, cm^{-1}						
1	6.1	2.45	528		613	763	875	914	995
2	7.0	5.90	527		613	762	875	915	993
3	8.0	2.62	527	567	613	753	875	915	995
4	9.0	0.84		568	610	745	875		
5	10.0	0.69		565		745	875		
6	6.3	2.0	520		608	761	878		

[a] Solution 6 is 4.0 M in F^-. All bands are polarized with the exception of the 915-cm^{-1} band.

Table II. Raman Spectra of Solid Borates[a]

Material	Frequencies, cm^{-1}
HBO_2 orthorhombic	401 (1), 415 (1), 475 (1), 595 (10), 809 (3)
HBO_2 monoclinic	428 (2.3), 475 (3.5), 518 (2.3), 533 (3.5), 782 (10)
HBO_2 melt 220 °C	595, 805
Anhydrous $NaBO_2$	472 (2), 623 (10), 680 (2.4), 767 (2)
$NaB_5O_8 \cdot 5H_2O$	488 (2), 527 (10), 770 (3), 920 (3.5)
$Na_2B_4O_7 \cdot 10H_2O$	383 (1), 460 (1), 573 (10), 865 (1), 945 (1)
$Mg(BO_2)_2 \cdot 3H_2O$ (pinnoite)	740
$Na_3B_3F_6O_3$	350 (2), 378 (2), 595 (10), 730 (3), 1060 (0.5)

[a] Numbers in parentheses indicate relative intensities.

Results and Discussion

Polyborate Ions. The Raman spectra of solutions containing H_3BO_3–NaOH are reproduced in Figure 2. The main frequencies are listed in Table I. The Raman spectra of reference solids and that of metaboric acid melt are described in Table II.

The frequencies of the ν_1 bands of boric acid and borate ion are 875 and 745 cm^{-1}, respectively, and have already been reported.[6,12]

Pentaborate Ion. The presence of pentaborate ion is evident in the solutions at pH 6.1, 7.0, and 8.0. The identification of this ion is based on the close correspondence of the frequencies at 527, 763, and 914 cm^{-1} with the position and relative intensities of the bands in the spectrum of solid $NaB_5O_8 \cdot 5H_2O$.

Triborate Ion. The band at 613 cm^{-1} observable in the solutions from pH 6.1 to 9.0 is assigned to an ion containing the boroxine ring. The assignment is based on the similarity of this absorption with the lines observed for orthorhombic metaboric acid and anhydrous sodium metaborate, both known from single crystal x-ray diffraction analysis[15,16] to contain the boroxine core. Goubeau and Keller[17] have analyzed the Raman spectra of a number of molecular compounds containing a trisubstituted boroxine ring. These compounds show a typical pattern of three polarizable bands, ν_1, ν_2, and ν_3, at about 1200, 800, and 500 cm^{-1}. Boric oxide glass also shows this pattern. A similar pattern would be expected for orthorhombic metaboric acid and anhydrous sodium metaborate in view of the structural similarities. In orthorhombic metaboric acid this pattern is partially discernible since it shows bands at 809 and 595 cm^{-1}; Parsons[18] has reported 819 and 598 cm^{-1} for these bands. The ν_1 band, expected at about 1200 cm^{-1}, is apparently too weak to be observed, possibly due to strong hydrogen bonding in the lattice. It was hoped that a melt would show the ν_1 band but the spectrum was very noisy and the only observable bands were at 595 and 805 cm^{-1}. In the case of anhydrous sodium metaborate the strongest signal is observed at 623 cm^{-1}. The expected pattern is not present, possibly due to distortions in the ring which were detected in the x-ray diffraction study.[16] In the case of monoclinic metaboric acid the expected pattern is not observed. This can be understood since the crystal structure[19] as determined by x-ray diffraction analysis contains one of the boron atoms in the ring in a tetrahedral coordination, forcing considerable distortion. Furthermore the lattice consists of chains. There is a band at 995 cm^{-1} associated with the B_3 ion in solution which is polarized. This could correspond to the ν_1 vibration for this ion; on the other hand, there is no evidence of a ν_2 band. It is interesting to note that the B_3 ion spectrum resembles that of a trisubstituted boroxine ring in showing what appears to be a strong ν_3 at 613 cm^{-1}, also polarized, and an apparent ν_1 band in spite of the fact that the symmetry has to be altered by conversion of one of the boron atoms to tetrahedral coordination to accommodate for the charge in the ion. It is possible, however, that the ion could be planar.

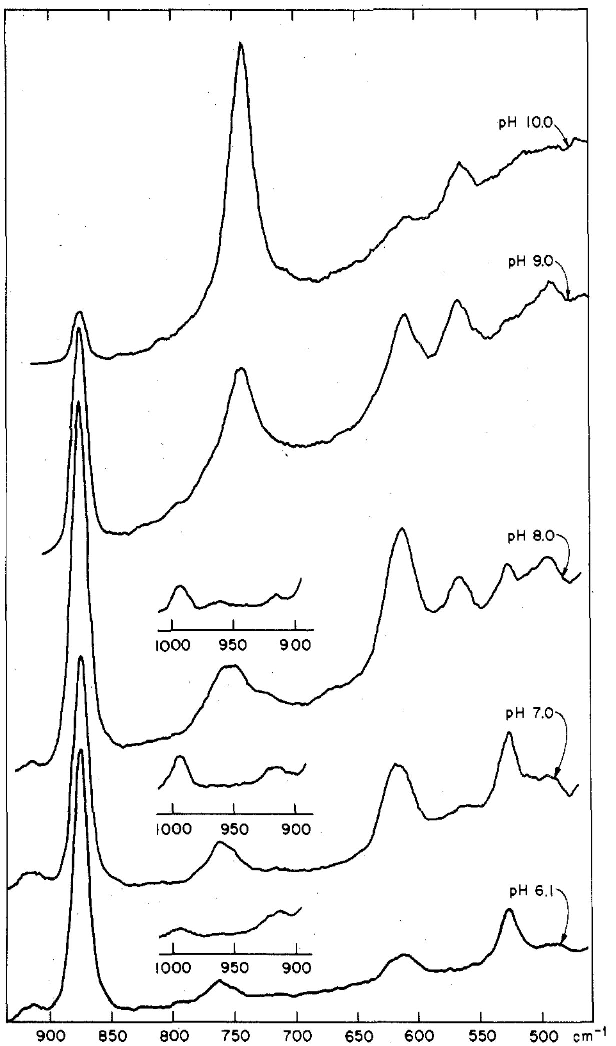

Figure 2. Raman spectra of solutions containing polyborate ions.

Tetraborate Ion. The tetraborate ion is identified in solution on the basis of a line at 567 cm^{-1} which is close to the main absorption observed at 573 cm^{-1} for solid tetraborate decahydrate. Other lines in solid tetraborate cannot be identified in the solutions due to their inherent weakness and the relatively low concentration of tetraborate ion in solution.

The presence of a (2,1) ion cannot be established since the main absorption for such an ion, if similar to pinnoite, would fall under the absorption of $B(OH)_4^-$ ion. It seems from the pH titration data that this species is not important at ambient temperature. Observation of the spectra shows that the

Table III. Relative Proportion of Tetrahedral Boron in Polyborate Ions[e]

pH	[B],[a] M	[Na],[a] M	$[H_3BO_3]$,[b] M	$[NaB(OH)_4]$,[b] M	Polyborate[c] [B], M	Polyborate[c] [Na], M	Tetrahedral boron,[d] %
6.1	2.45	0.425	0.806 ± 0.01		1.64	0.425	25.9
7.0	5.90	1.505	0.763 ± 0.01		5.137	1.505	29.3
8.0	2.62	0.785	0.402 ± 0.002		2.218	0.785	35.4
9.0	0.84	0.345	0.143 ± 0.003	0.105 ± 0.003	0.592	0.240	40.5
10.0	0.69	0.505	0.041 ± 0.001	0.349 ± 0.008	0.300	0.156	52.0

[a] Titration values. [b] Spectrophotometric values. [c] Difference between values given in *a* and *b*. [d] Na value in *c* × 100/[B] value in *c*. Values are accurate to about ±1%. [e] All concentrations expressed as mol/l.

pentaborate line at 763 cm^{-1} gradually disappears with increasing pH and collapses into the 745-cm^{-1} band due to borate ion.

The identification of pentaborate, triborate, and tetraborate in the solutions serves as confirmation and is mutually supportive of the results obtained by Ingri[1,2] and Mesmer et al.[3] on the basis of electrometric titrations and also of those based on NMR studies[20,21] which offered indirect evidence for the identity of the ions.

One of the shortcomings of the pH titration method is that, although it gives reliable information about the number of boron atoms per ion, the charge is somewhat less certain. It was realized that information about the charge on the ions could be derived by establishing an average proportion of tetrahedral boron for the ions which reflects their charge. This average tetrahedral boron is simply determined by obtaining the ratio of sodium to boron on the ions. Table III gives this information. It is seen that the proportion of tetrahedral boron increases with pH from a value of 25.9 to about 50%. Extrapolation of these values to lower pH gives a tetrahedral boron of about 20% at pH 5.0. It is also observed that the concentration of polyborate ions peaks at about a pH of 7.0. The concentration of polyborate ions at pH 5.0 was estimated to be 0.1 M in B and was too uncertain to calculate the proportion of tetrahedral boron at that pH. These values are a strong indication that both pentaborate and triborate are univalent containing 20 and 33% tetrahedral boron, respectively, and tetraborate is divalent containing 50% tetrahedral boron. The increase in the proportion of tetrahedral boron with pH correlates also with the order of appearance of each ion as observed in the spectra, pentaborate being first followed by triborate and tetraborate, and appears as a predictable distribution since the increase in OH$^-$ concentration would tend to increase attack of neutral trigonal boron and conversion to charged tetrahedral boron. There is a close parallel in the anhydrous system $Na_2O{\cdot}B_2O_3$ studied by Bray et al.[22] using NMR. It was found that the conversion of trigonal boron to tetrahedral boron is a function of increasing alkali oxide concentration.

There is no evidence from the spectra or the determination of the relative proportion of tetrahedral ion for the formation of a (3.2) ion which would be a divalent triborate ion containing 66% tetrahedral boron. The spectrum of such species would probably show a significant shift of the main frequency due to the presence of an additional hydroxyl group in the ion. This effect was not observed. Ingri considered the (3,2) ion since it improved the fit of the experimental data[2] in some of the studies; however, the data obtained in 3.0 M KBr did not require this species.

Apparently there is a discontinuity in the tetrahedral boron distribution beyond 50% and increased alkalinity converts tetraborate ion (50% tetrahedral boron) directly to borate $B(OH)_4^-$ ion (100% tetrahedral boron).

Approximate values for the equilibrium quotients for the formation of these ions were derived from the data at pH 7.0 and 10.0. Agreement with Ingri's values is reasonable, considering that the solutions are far from ideal for the determination of equilibrium constants. The results are given below:

Ingri's values[2]

$$\log \beta_{31} = \frac{[B_3O_3(OH)_4^-][H^+]}{[H_3BO_3]^3} = -6.6 \pm 0.1 \qquad -6.84$$

$$\log \beta_{51} = \frac{[B_5O_6(OH)_4^-][H^+]}{[H_3BO_3]^5} = -6.9 \pm 0.1 \qquad -6.77$$

$$\log \beta_{42} = \frac{[B_4O_5(OH)_4^{2-}][H^+]^2}{[H_3BO_3]^4} = -15.6 \pm 0.1 \qquad -14.66$$

Fluoropolyborate Ions. The Raman spectrum of a 0.66 M solution of $Na_3B_3F_6O_3$ is given in Figure 3. Initially it was concluded in observing lines at 875 and 760 cm^{-1} that these were due to H_3BO_3 and BF_3OH^- resulting from the depolymerization of the $B_3F_6O_3^{3-}$ ion occurring as described by the following reactions

$$Na_3B_3F_6O_3 + 3H_2O \rightleftarrows 3NaBF_2(OH)_2 \tag{1}$$

$$2NaBF_2(OH)_2 \rightleftarrows NaBF_3OH + H_3BO_3 + NaF \tag{2}$$

This situation would not be surprising since tetraborate is depolymerized in water into H_3BO_3 and $B(OH)_4^-$. Hibben[6] observed this behavior on the basis of Raman spectra.

The stoichiometry of the depolymerization required that sodium fluoride, not observed in Raman, would be formed. This suggested an experiment whereby boric acid, sodium fluoride, and sodium hydroxyfluoroborate dissolved in equivalent proportions should generate the same spectrum as aqueous $Na_3B_3F_6O_3$. This was the case, indeed; furthermore, evaporation of that solution yielded pure $Na_3B_3F_6O_3$ as established by elemental analysis, ir, alkalimetric titration, and the x-ray powder diffraction pattern. This experiment proved the reversibility of the equations described above and gave an alternate and simpler method to obtain the complex salt. In spite of the straightforward chemistry described above, closer scrutiny of the Raman spectrum revealed some inconsistencies. Pure $NaBF_3OH$ absorbs at 763 cm^{-1} and the 760-cm^{-1} band actually observed appeared to be asymmetric. The presence of a band at 610 cm^{-1} was also detected. The intensity of this band proved to be temperature dependent, increasing at lower temperatures. This suggested more species than those originally assumed. The ^{19}F NMR spectrum, Figure 4, revealed the presence of a considerable proportion of species containing a F/B ratio of 2.0. This was concluded from the presence of a strong signal with a chemical shift (reference C_6F_6) of −29.6 ppm, corresponding quite closely to the value assigned by Mesmer et al.[23] to species with a F/B ratio of 2.0. The signal at −22.9 ppm corresponds to BF_3OH^- and the small spike at −16.1 ppm corresponds to BF_4^-. The spectral evidence indicates that the equilibria described in eq 1 and 2 are not shifted completely to the right and that there are considerable amounts of $BF_2(OH)_2^-$ and $B_3F_6O_3^{3-}$ ions present. Analysis of the 760-cm^{-1} band with a curve resolver revealed two components at 763 and 753 cm^{-1}, the first being due to BF_3OH^-, as assigned on the basis of pure $NaBF_3OH$, and the second due to $BF_2(OH)_2^-$. The frequency of the ν_1 band of $BF_2(OH)_2^-$ fits the correlation between frequency of this

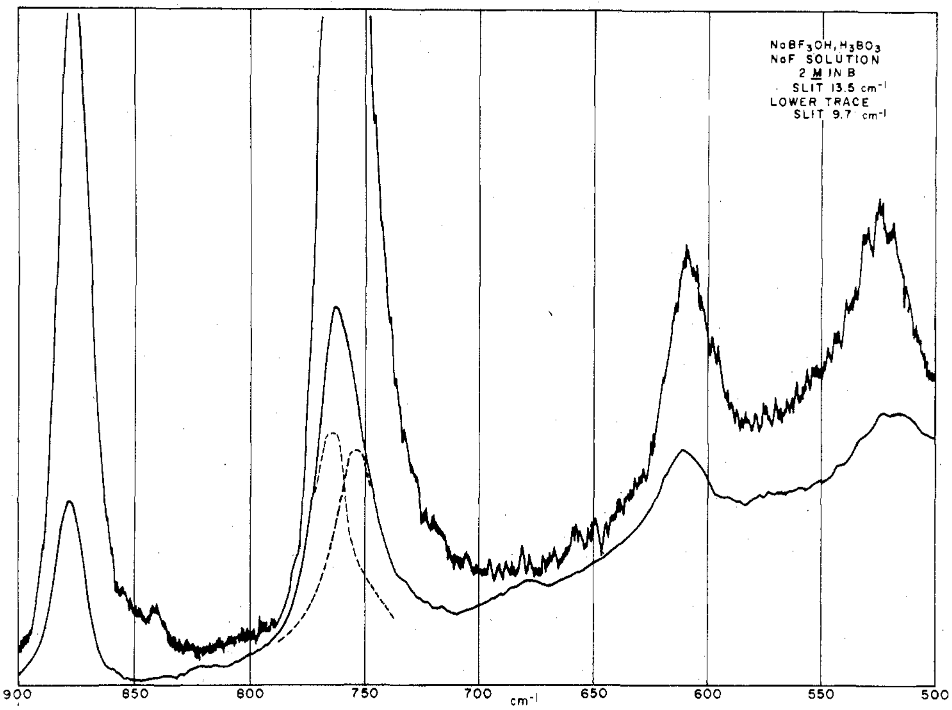

Figure 3. Raman spectrum of a solution containing fluoropolyborate ions.

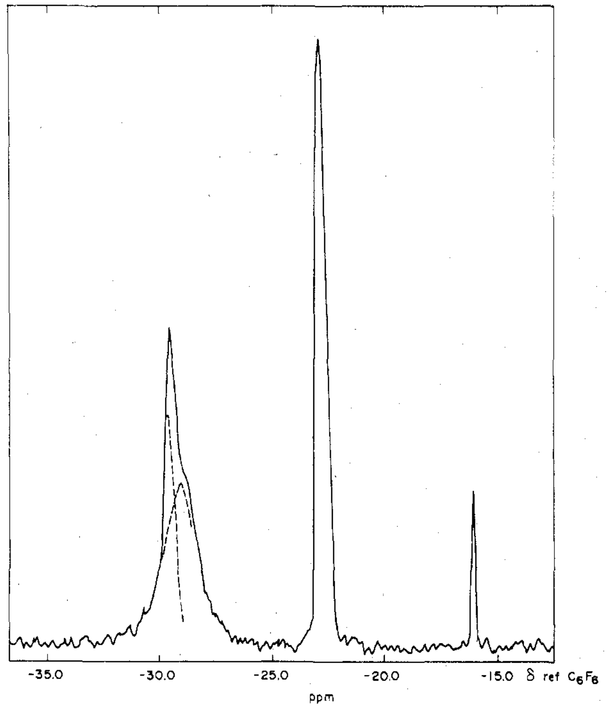

Figure 4. ^{19}F NMR at 0 °C of a solution containing fluoropolyborate ions. Solution is 2 M in boron with a F/B of 2.

absorption and the degree of substitution of fluorine by hydroxyl in substituted fluoroborates; thus BF_4^- absorbs at 770 cm^{-1}, BF_3OH^- at 763 cm^{-1}, $BF_2(OH)_2^-$ at 753 cm^{-1}, and $B(OH)_4^-$ at 745 cm^{-1}. Similarly analysis of the ^{19}F NMR signal at −29.6 ppm (reference C_6F_6) revealed two signals one due to $BF_2(OH)_2^-$ and the other apparently due to $B_3F_6O_3^{3-}$. The presence of $B_3F_6O_3^{3-}$ is confirmed by the band at 610 cm^{-1} in the Raman spectrum. This line corresponds to the line at 595 cm^{-1} observed in the spectrum of the solid. It is interesting to note the similarity in the frequencies of the bands of $Na_3B_3F_6O_3$ and metaboric acid. This apparently is an indication of the presence of a boroxine ring.

A semiquantitative material balance, based on the intensities of the ^{19}F NMR and a calibration of the $B(OH)_3$ and $NaBF_3OH$ lines in the Raman spectrum, gives the following approximate distribution for a 2 M in B solution prepared by dissolving equimolar amounts of $NaBF_3OH$, NaF, and H_3BO_3.

	BF_3OH^-	$BF_2(OH)_2^-$	$B_3F_6O_3^{3-}$	F^-	H_3BO_3
Approx molarity	0.5	0.5	0.2	0.5	0.2

Free fluoride is not shown in the spectrum given in Figure 4; it absorbs at about −44 ppm and it is not resolved from $BF(OH)_3^-$,[23] thus being a potential source of error in the balance.

Acknowledgment. Chemical and x-ray analyses were provided by W. R. Laing and H. W. Dunn of the Oak Ridge National Laboratory Analytical Chemistry Division. The NMR spectra were kindly run by A. Rutenberg. I wish to thank G. Begun for useful advice in running the Raman spectra and C. Baes, Jr., and R. Mesmer for helpful discussions. I reiterate my appreciation of the help provided by the Smithsonian Institution in lending a sample of pinnoite. Research sponsored by the Energy Research and Development Administration under contract with Union Carbide Corporation.

Registry No. $B_5O_6(OH)_4^-$, 17927-69-4; $B_3O_3(OH)_4^-$, 17927-68-3; $B_4O_5(OH)_4^{2-}$, 12344-83-1; $B_3O_3F_6^{3-}$, 59753-06-9; HBO_2, 13460-50-9; $NaBO_2$, 7775-19-1; $NaB_5O_8\cdot5H_2O$, 12046-75-2; $Na_2B_4O_7\cdot10H_2O$, 1303-96-4; $Mg(BO_2)_2\cdot3H_2O$ (pinnoite), 14916-49-5; $Na_3B_3F_6O_3$, 19052-40-5.

References and Notes

(1) N. Ingri, *Acta Chem. Scand.*, **17**, 573 (1963), and references therein.
(2) N. Ingri, *Acta Chem. Scand.*, **17**, 581 (1963).
(3) R. E. Mesmer, C. F. Baes, Jr., and F. H. Sweeton, *Inorg. Chem.*, **11**, 537 (1972).
(4) C. L. Christ, *Am. Mineral.*, **45**, 334 (1960).
(5) J. O. Edwards and V. Ross, *J. Inorg. Nucl. Chem.*, **15**, 329 (1960).
(6) J. H. Hibben, *Am. J. Sci.*, 113 (1938).
(7) A. W. Laubengayer and R. D. Rosenstein, Symposium on Complex Ions and Polyelectrolytes, Cornell University, Ithaca, N.Y., 1951.
(8) R. E. Mesmer, private communication.
(9) R. E. Mesmer, K. M. Pallen, and C. F. Baes, Jr., *Inorg. Chem.*, **12**, 89 (1973).
(10) I. G. Ryss, *Dokl. Akad. Nauk SSSR*, **97** (4), 691 (1954).
(11) M. V. Aknmanova and G. E. Kurilchikova, *Opt. Spektrosk.*, **8**, 498 (1960).

(12) J. O. Edwards, G. C. Morrison, V. F. Ross, and J. W. Schulz, *J. Am. Chem. Soc.*, **77**, 266 (1955).
(13) F. C. Kracek, G. W. Morey, and H. E. Merwin, *Am. J. Sci.*, 143 (1938).
(14) S. Pawlenko, *Z. Anorg. Allg. Chem.*, **315**, 147 (1962).
(15) C. R. Peters and M. E. Milberg, *Acta Crystallogr*, **17**, 229 (1964).
(16) M. Marezio, H. A. Plettinger, and W. H. Zachariasen, *Acta Crystallogr.*, **16**, 594 (1963).
(17) J. Goubeau and H. Keller, *Z. Anorg. Allg. Chem.*, **272**, 303 (1953).
(18) J. L. Parsons, *J. Chem. Phys.*, **33**, 1860 (1960).
(19) W. H. Zachariasen, *Acta Crystallogr.*, **16**, 385 (1963).
(20) R. K. Momii and N. H. Nachtrieb, *Inorg. Chem.*, **6**, 1189 (1967).
(21) H. D. Smith, Jr., and R. J. Wiersema, *Inorg. Chem.*, **11**, 1152 (1972).
(22) P. J. Bray and J. G. O'Keefe, *Phys. Chem. Glasses*, **4**, 37 (1963).
(23) R. E. Mesmer and A. C. Rutenberg, *Inorg. Chem.*, **12**, 699 (1973).

Contribution from the Department of Chemistry,
University of Pittsburgh, Pittsburgh, Pennsylvania 15260

Solubility of Hydrogen in Intermetallics Containing Rare Earth and 3d Transition Metals

C. A. BECHMAN, A. GOUDY, T. TAKESHITA, W. E. WALLACE,* and R. S. CRAIG

Received November 5, 1975 AIC50795C

Pressure–composition isotherms have been determined for the systems RCo_3–H and RFe_3–H, with R = Gd, Tb, Dy, and Ho, and also for $ErFe_3$–H. The studies show certain systematics in regard to the affinity of the alloy for hydrogen: (1) it is greater for the Fe compounds than for the corresponding Co compounds; (2) it decreases as the atomic number of R increases; (3) it increases with increased rare earth content of the compound. The systematic trends are thought to be brought on by systematic variations in the band structure produced by variations in composition and stoichiometry. The hydrogen storage capacities of the RT_3 phases (T = Fe or Co) exceed those of the RCo_5 phases and the well-known hydrogen absorber $LaNi_5$. The amount of hydrogen stored at pressures of 400 psi ranges from about 4 to 6×10^{22} atoms/cm^3; some of these exceed the particle density of liquid hydrogen, 4.2×10^{22} atoms/cm^3.

Introduction

A number of RT_5 compounds[1-3] (R is a rare earth and T is Co or Ni) have been found to absorb and desorb rapidly relatively large quantities of hydrogen, some under moderate pressures and at room temperature. Buschow and Van Mal[4] have shown that a shift in the stoichiometry of $LaNi_5$ in the nickel-poor direction results in an increase in the quantity of hydrogen absorbed by the material at a reduced pressure. Structurally, RT_3 compounds may be considered[5] to be T-deficient RT_5 phases; hence, it is of considerable interest to examine these materials as hydrogen absorbers for comparison with the RT_5 phases and the T-deficient RT_5 phases.

In a previous communication we reported hydrogen absorption data for $ErCo_3$ and some information for the $DyCo_3$–H and $HoCo_3$–H systems.[3] This study has been extended in the present work to include $TbCo_3$ and $GdCo_3$ and also the corresponding RFe_3 series. Additional results for the Dy- and Ho-containing ternaries are also presented.

In the comprehensive study of the RCo_5 series as H_2 absorbers carried out by Kuijpers,[6] a systematic trend was noted: the hydrogen vapor pressure measured at a given temperature and at a fixed H:RCo_5 ratio increased with increasing atomic number of R, indicating a decreasing affinity for hydrogen as the atomic number of R is increased. The lanthanide contraction is operative in the RCo_5 sequence so that the observation of Kuijpers is equivalent to a correlation between affinity for H_2 and the size of the RCo_2 unit cell. In the phase based on the composition $LaNi_5$ the volume of the unit cell decreases as the sample departs from ideal stoichiometry in the nickel-rich direction. The results of Buschow and Van Mal[4] referred to above also show a direct relationship between affinity of the metal for H_2 and the size of the unit cell. The RFe_3 phase has larger unit cell dimensions than the corresponding RCo_3; therefore, if the systematics observed by Kuijpers and by Buschow and Van Mal hold, it might be expected that the affinity for H_2 would be in the order $RFe_3 > RCo_3$. To ascertain whether this was indeed the case was one of the motivations for the present study. In addition, we were interested in the general behavior of these two series of materials as solvents for H_2 and also in any other systematic characteristics that they might exhibit which would shed light on the truly extraordinary features of the RT_x systems—their ability to contain large amounts of hydrogen and the great rapidity with which they absorb and release hydrogen.

Experimental Section

Samples were prepared by induction melting the constituent metals in a water-cooled copper boat under a purified argon atmosphere. The metals used were the highest purity materials commercially available: cobalt >99.999%, iron >99.999% and rare earths >99.9%, exclusive of gaseous impurities. After melting, the samples were annealed and homogenized in the cold boat so that no additional phases could be detected when subjected to x-ray analysis. The hydriding system was constructed of stainless steel. The temperature of the sample was controlled by a stirred water bath below 100 °C and by an electric furnace above that temperature. The water bath was controlled to within 0.1 °C and the furnace to within 0.25 °C.

The samples were crushed to less than 1-mm particle size in air before being placed in the sample holder. They were then activated by allowing them to sequentially absorb and desorb hydrogen until the quantity of hydrogen absorbed became constant. The absorption process was conducted at pressures up to 1500 psig and was usually complete after about 2 min; however, at least 2 h was allowed for the system to reach equilibrium since this step is strongly exothermic. The desorption was accomplished by allowing the hydrogen to flow out through water into an inverted buret to atmospheric pressure, followed by pumping on the sample with a mechanical pump. During the final stage of pumping the temperature of the sample was increased to about 250 °C.

Desorption pressure–composition isotherms were determined by first measuring in a known quantity of H_2 and then removing measured quantities of hydrogen from the system and establishing the resulting pressure at equilibrium. The dead spaces in the hydriding system had been calibrated and appropriate allowance was made for H_2 remaining in the dead spaces. Time to reach equilibrium varied from 0.5 to 2 h above atmospheric pressure but up to 12 h below. Absorption pressure–composition isotherms were established by metering in fixed amounts of H_2 and waiting for the pressure to become constant between additions. Allowance was again made for the dead space H_2. Ashcroft test gauges were used for pressure measurements above